Building and Environment 46 (2011) 245–252

Contents lists available at ScienceDirect

Building and Environment

journal homepage: www.elsevier.com/locate/buildenv

Modeling deposition of particles in vertical square ventilation duct flows

Ran Gao, Angui Li*

School of Environmental and Municipal Engineering, Xi'an University of Architecture and Technology, 710055, Shaanxi, Xi'an, PR China

ARTICLE INFO

Article history:
Received 20 May 2010
Received in revised form
19 July 2010
Accepted 20 July 2010

Keywords:
Particles
Ventilation ducts
Computational fluid dynamics
Lagrangian eddy lifetime model
Dimensionless deposition velocities of particles
Reynolds-averaged Navier–Stokes equations

ABSTRACT

The presence, flow, and distribution of particle in heating, ventilation, and air-conditioning (HVAC) ducts influence the quality of air in buildings and hence the health of building occupants. To shed a better light on the flow of particles in HVAC ducts this a paper has considered the effects of drag, lift force, gravity, Brownian diffusion, and turbulent diffusion on the dimensionless deposition velocity of particles in smooth vertical ventilation ducts using fully developed and developing velocity profiles. Based on the Reynolds stress transport model (RSM) at two different air velocities, 3.0 m/s and 7.0 m/s, the aforementioned effects were predicted using Reynolds-averaged Navier–Stokes (RANS)–Lagrangian simulation on square shaped ducts under vertical flows.

Preliminary results suggest that the gravity of particles does not directly change the dimensionless deposition velocity in vertical flows. Nevertheless, the gravity of particles contributes to changing the Saffman lift force. It is thus the Saffman lift force that directly changes the dimensionless deposition velocity of particles in vertical flows. In addition, the difference in the dimensionless deposition velocities between fully developed and developing flows is owing to the turbulent diffusion, turbulent intensity, and needless to say, the Saffman lift force under different dimensionless particle relaxation time.

1. Introduction

The mechanisms of deposition of particle in ducts can be applied to a number of fields including contaminants control, filtration, and aerosol sampling. Particle deposition can influence the size distribution of particles along ducts as a result of drag, lift force, gravity, Brownian diffusion, and turbulent diffusion. Knowing the particle size distribution in ducts can help estimate the exposure of building occupants in HVAC-supported buildings.

Size distributions of deposited particles in HVAC ducts have not been fully investigated. One study showed that the total mass of the deposited particles in an HVAC duct was likely to be dominated by large particles, debris, and fibers [1]. Other studies have reported that particle deposition alters the quality of indoor air in HVAC-based buildings. M.S. Zuraimia (2007) and Chaosheng Liu (2006) suggested that particle deposition on the interior surfaces of ducts can lead to more microorganisms and secondary pollutants generations hence affecting the quality of indoor air occupants breathe [2,3]. In addition, for small size ducts, particle deposition reduces the airflow rate and hence degrades the efficiency of the ventilation system. Therefore, predicting particle deposition in HVAC ducts is important to improve the indoor air quality, and to increase the efficiency of the ventilation system.

Particle deposition on the HVAC ducts of the History Museum in Shaanxi, China was investigated by our research team. The average density of particles studied was 1800 kg/m^3. It was found that the distribution frequency of deposited particles lesser and larger than 10 μm in diameter was 55% and 45%, respectively. Since particles with different diameters have different aerodynamics mechanisms, our research team has studied the deposition of particles diameters smaller than 10 μm (0.1–10 μm) in both horizontal and vertical ducts [4]. The research team has also investigated deposition of particles larger than 10 μm (10–200 μm) in horizontal ducts [5,6]. In this paper, we will focus on the deposition of particles ranging from 10 to 200 μm in vertical ducts.

Uijttewaal and Oliemans (1996) performed Lagrangian simulation of particle deposition in the inertia-moderated regime in vertical cylindrical-tube flows generated by both direct numerical simulation (DNS) and large eddy simulation (LES) [7]. Zhang and Ahmadi (2000) analyzed particle deposition on vertical and horizontal floor surfaces in a directly numerical simulation (DNS) generated channel flow [8]. The latter study is the only DNS Lagrangian simulation that includes deposition of particles on a horizontal floor surface. However, few investigations have been found using Lagrangian simulation to study the deposition mechanism in vertical ducts with the analysis of gravity, lift force and turbulent development.

Over the past two decades, empirical equations, Eulerian models and Lagrangian simulations were developed to predict

* Corresponding author. Tel.: +86 29 82202507; fax: +86 29 82202729.
E-mail address: liag@xauat.edu.cn (A. Li).

0360-1323/$ – see front matter © 2010 Elsevier Ltd. All rights reserved.
doi:10.1016/j.buildenv.2010.07.020

Nomenclature

α	cross dimension of the duct
C	instantaneous particle concentration
$\overline{C}$	time-averaged particle concentration
C_{ave}	time-averaged airborne particle concentration in ventilation ducts
C_c	slip correction factor
C_D	drag coefficient
d_p	particle diameter
D_h	hydraulic diameter of the duct
D_B	particle Brownian diffusivity
f	Fanning friction factor
J	time-averaged particle flux to the surface
J_B	Brownian diffusive particle flux
k	fluctuation kinetic energy
L	duct section length
N_{dep}	particle deposition numbers to wall
N_{in}	total particle numbers at a duct inlet
$\overline{p}$	mean pressure
R_{ij}	Reynolds stress tensor
t	time
T	integral time scale
T_L	fluid Lagrangian integral time
T_e	eddy lifetime integral time
u_i'	the ith fluctuation velocity component
u_i	instantaneous velocity
u	fluid phase velocity
u_p	particle velocity
u_{px}	particle velocity in the axial direction
u^*	friction velocity
V_d	deposition velocity
V_d^+	dimensionless deposition velocity
$\overline{u}_i$	mean velocity
U_{ave}	air average velocity in the duct
x_i	position

Greek symbols

ε	turbulence dissipation rate
λ	the mean free path of gas molecules
μ	molecular viscosity of the fluid (dynamic viscosity of air)
ρ	constant mass density (air density)
ρ_p	density of the particle
τ^+	dimensionless particle relaxation time
ς	normally distributed random number
ξ_p	eddy diffusivity of the particle

particle deposition with turbulent flows in tubes, pipes or ducts. Lagrangian simulation is one of the main approaches for the prediction of deposition velocity of particles in turbulent flow. The results of Lagrangian simulation of particle deposition are consistent with that of the experiment in both magnitude and tendency [9,10].

In Lagrangian simulation, it is usually assumed that the motion of particles in the fluid does not affect the structure of the turbulent flow. It means that the fluid affects the particle momentum, but the particles have no influences on the fluid momentum. This assumption is termed the one-way coupling assumption [11–14].

This paper has considered the effects of drag, lift force, gravity, Brownian diffusion, and turbulent diffusion on the dimensionless deposition velocity of particles in smooth ventilation ducts using fully developed and developing velocity profiles. Based on the Reynolds stress transport model (RSM) at two different air velocities, 3.0 m/s and 7.0 m/s, the aforementioned effects were predicted using Reynolds-averaged Navier–Stokes (RANS)–Lagrangian simulation on square shaped ducts under.

2. Numerical method

In this study, we use the one-way coupling RANS-Lagrangian to model particle deposition. . Both fully developed and developing velocity profiles in smooth vertical ventilation ducts are considered in the simulation. The duct is square with cross-section of 0.3 m × 0.3 m and 0.1 m × 0.1 m. They are typical in the HAVC systems. The diameters of the predicted particles are 10, 15, 20, 30, 40, 50, 70, 80, 100, 120, 150, 180, and 200 μm. The particle deposition is expected to be uniform over the entire internal duct [4–8].

The turbulence model in this simulation is Reynolds stress transport model (RSM) with linear pressure-strain and standard wall functions. Turbulent diffusion model and eddy lifetime model are introduced to simulate dispersion phase. Concerning the lift force derived by Saffman (1965, 1968) [15,16], gravity, Brownian diffusion, drag and turbulent diffusions, the simulation analyzes the influence of these factors on the deposition velocity of the particles.

2.1. Simulation of the turbulent airflow field

2.1.1. Turbulent airflow model

The air in the ventilation ducts can be regarded as a three dimensional, incompressible, stable, isothermal, turbulent and continuous fluid, which is governed by conservation laws of mass and momentum, and continuity equations and momentum conservation equations for the mean motion of the particles are as follows:

Continuity equation:

$$\frac{\partial \overline{u}_i}{\partial x_i} = 0 \tag{1}$$

Momentum conservation equations:

$$\overline{u}_j \frac{\partial \overline{u}_i}{\partial x_j} = -\frac{1}{\rho}\frac{\partial \overline{p}}{\partial x_i} + \frac{\mu_t}{\rho}\frac{\partial^2 \overline{u}_i}{\partial x_j \partial x_j} - \frac{\partial}{\partial x_j} R_{ij} \tag{2}$$

where $\overline{u}_i$ is the time-averaged mean stream-wise air velocity, x_i is the position, ρ is the constant mass density (air density), μ is the dynamic viscosity, μ_t is the turbulent viscosity, and $R_{ij} = \overline{u_i' u_j'}$ is the Reynolds stress tensor. Here, $u_i' = u_i - \overline{u}_i$ is the ith fluctuation velocity component.

In this study, we used the Reynolds stress transport model (RSM) as the turbulence model to render the Reynolds-Averaged Navier–Stokes (RANS) equations solvable by adding twelve transport equations for the Reynolds stress along with an equation for the dissipation rate [17–19].

2.1.2. Boundary conditions

The boundary conditions of fully developed flow of the inlet and outlet in the simulation are periodic boundary conditions which are used in the initial flow field computation [7]. After initial flow field computation, discrete phase model is introduced to model the motion of particles. No-slip boundary conditions are employed to the walls. In addition, boundary conditions of developing flow are the same while modeling the fully developed flow except at the inlet and outlet of the duct, where we adopt velocity-inlet and pressure-outlet boundary conditions instead of periodic boundary conditions.

2.2. Dispersion phase model

2.2.1. Turbulent diffusion model of the particle

Prediction of particle dispersion employs the concept of integral time scale, T, which describes the time spent on turbulent motion along the particle path and is given by [20]:

$$T = \int_0^\infty \frac{u_p'(t)u_p'(t+s)}{\overline{u_p'^2}}\mathrm{d}s \tag{3}$$

The integral time is proportional to the particle dispersion rate, as larger values indicate more turbulent motion in the flow. For small "tracer" particles that move with the fluid (zero drift velocity), the integral time, T, becomes the fluid Lagrangian integral time, T_L. When the Reynolds stress model (RSM) is used, this time scale can be approximated as,

$$T_L \approx 0.3\frac{k}{\varepsilon} \tag{4}$$

2.2.2. Eddy lifetime model

The flow in ventilation duct in this paper is turbulent. To predict the dispersion of the particles due to turbulence, we use eddy lifetime model. The eddy lifetime model of particles is the Lagrangian stochastic model used to trace the trajectory of the particle in the duct flow. According to the initial conditions that define the starting positions, velocities and particle diameters, the motion of single particle can be calculated [21].

The interaction of a particle with a succession of discrete fluid phase turbulent eddies is simulated. Each eddy is characterized by Gaussian distributed random velocity, u_i' and fluctuation and eddy lifetime time scale, T_e.

The values of u_i' are sampled by assuming that they obey a Gaussian probability distribution, which is given by [21]:

$$u_i' = \varsigma\sqrt{\overline{u_i'^2}} \tag{5}$$

where ς is a normally distributed random number and the remainder of the right-hand side is the local RMS value of the velocity fluctuations. Since the kinetic energy of turbulence is known at each point in the flow, these values of the RMS fluctuating components can be obtained (assuming isotropy) as

$$\sqrt{\overline{u_i'^2}} = \sqrt{\frac{2k}{3}} \tag{6}$$

The characteristic lifetime of the eddy is defined as a constant:

$$T_e = 2T_L \tag{7}$$

where T_e is eddy lifetime time scale and T_L is given by Eq. (4).

2.2.3. Initial and boundary conditions of the particles

The primary input for the particle phase calculations are the initial conditions that include the starting positions, velocities and particle diameters. It is assumed that 10^5 discrete particles are released into the duct and are distributed uniformly at the inlet of the duct [4–6]. Two different kinds of particles whose densities are 1800 kg/m^{3}and 800 kg/m^3 respectively are introduced into the simulation.

The air and particle are assumed at 25 °C and an atmospheric pressure (101,325 Pa). Particle concentrations in HVAC ducts are supposed to be low enough to ignore interaction between particles. The ducts are assumed to be a perfect sink so that once a particle contacts the wall; it does not bounce or detach and adhere to the wall [7].

Given initial conditions of velocity and position, the motion of a single particle is calculated by treating it as a series of interactions with discrete eddies having a characteristic size, lifetime and velocity.

2.2.4. Motion equations of particle

Considering drag, gravitational setting, Saffman lift force and turbulent diffusions in the process of computation, Motion equations of the particle can be written (for the x direction in Cartesian coordinates) as:

$$\frac{\mathrm{d}u_p}{\mathrm{d}t} = F_D(u-u_p) + \frac{g_x\left(\rho_p-\rho\right)}{\rho_p} + F_x \tag{8}$$

where $F_D(u-u_p)$ is the drag force per unit particle mass and

$$F_D = \frac{18\mu}{\rho_p d_p^2}\frac{C_D\mathrm{Re}}{24} \tag{9}$$

where, u is the fluid phase velocity, u_p is the particle velocity, ρ is the air density, ρ_p is the density of the particle, d_p is the particle diameter and μ is the molecular viscosity of the fluid. C_D and Re is drag coefficient and relative Reynolds number respectively [22].

2.2.5. Particle transport mechanisms

Forces and mechanisms influencing particle motion are potentially present in turbulent ventilation duct flow. This paper has considered the effects of drag, lift force, gravity, Brownian diffusion, and turbulent diffusion on the particle deposition on ducts. The equations of those forces and mechanisms can be seen in Table 1.

The direction of the lift force depends on the relative velocity between the particle and the air in the x direction (stream-wise), evaluated at the particle center. A particle in a velocity gradient near a wall (where $\mathrm{d}u/\mathrm{d}y$ is positive) with a stream-wise velocity higher than the air velocity will experience a negative lift force, i.e., towards the wall. A particle that lags the air stream in the stream-wise direction has a lift force away from the wall.

Table 1
Particle transport mechanisms.

Particle transport mechanisms	Equations		References
Brownian diffusion	$J_B = -D_B\cdot\partial C/\partial y$	(10)	[4]
Turbulent diffusion	$J_{diff} = -(\xi_p + D_B)\cdot\partial C/\partial y$	(11)	[4]
Drag force	$F_d = \pi d_p^2\rho_a\lvert u-u_p\rvert(u-u_p)C_d/8C_c$	(12)	[4]
Gravitational force	$F_g = \pi/6d_p^3\rho_p g$	(13)	[4]
Shear-induced lift force	$F_l = 1.62\mu d_p^2(\mathrm{d}u/\mathrm{d}y)/\sqrt{\nu\lvert\mathrm{d}u/\mathrm{d}y\rvert}(u-u_{px})$	(14)	[22]

2.3. Particle deposition velocities

Deposition velocities are most commonly studied in the form of the dimensionless particle deposition velocity versus the dimensionless particle relaxation time.

2.3.1. Dimensionless particle deposition velocity

The dimensionless particle deposition velocity is defined by normalizing the dimensional deposition velocity with the friction velocity:

$$V_d^+ = \frac{V_d}{u^*} \tag{15}$$

where V_d^+ is the dimensionless deposition velocity, u^* is the friction velocity.

The deposition velocity, V_d, of a particle on a duct surface is defined as:

$$V_d = \frac{J}{C_{ave}} \tag{16}$$

where J is the time-averaged particle flux to the surface and C_{ave} is the time-averaged airborne particle concentration in the duct, evaluated at the centerline of the flow.

The friction velocity of turbulent duct flows, u^*, is defined as [23]:

$$u^* = U_{ave}\sqrt{f/2} \tag{17}$$

where f is the Fanning friction factor. For fully developed turbulent flow in a smooth duct, f is given by [24]:

$$\frac{1}{\sqrt{f}} = -3.6\log\left[\frac{6.9}{Re}\right] \tag{18}$$

where, Re is Reynolds number of the duct flow, based on the average flow velocity and the hydraulic diameter of the duct:

$$Re = \frac{D_h U_{ave}}{\nu} \tag{19}$$

here, ν is the kinematic viscosity of air, D_h is the hydraulic diameter of the duct, is defined as:

$$D_h = \frac{4A}{p} \tag{20}$$

A is the cross-sectional area of the duct and P is the perimeter of a section through the duct, normal to the direction of the flow.

According to the number of particles released to the inlet and the number of particles deposited on the floor, the deposition velocities to the surface of the vertical duct may be calculated as [25]:

$$V_{d,total} = -\frac{a\cdot U_{ave}\cdot\ln\left(1-\frac{N_{dep}}{N_{in}}\right)}{4\cdot L} \tag{21}$$

here, U_{ave} is the average air velocity in the axial direction, a is the cross dimension of the duct and L is the duct section length, $V_{d,total}$ is the surface deposition velocity, N_{dep} is the particle deposition number to the surface, N_{in} is total particle number at the inlet.

2.3.2. Dimensionless particle relaxation time

The dimensional relaxation time of a particle, τ_p, is the characteristic time for a particle velocity responding to changes of air velocity. It may be calculated for particles in the Stokes flow regime as follows

$$\tau^+ = \frac{C_c\rho_p d_p^2 u^{*2}}{18\mu\nu} \tag{22}$$

where C_c is the Cunningham slip correction factor, $\rho_p$is the particle density, d_p is the particle diameter and μ is the dynamic viscosity of air. The slip correction factor can be estimated by the expression

$$C_c = 1+\frac{2\lambda}{d_p}\left(1.257+0.4e^{-(1.1d_p/2\lambda)}\right) \tag{23}$$

where λ is the mean free path of gas molecules.

2.4. Calculation region and grid generation

Ventilation duct in this study is straight and vertical, and has a square cross-section. The ducts selected have two different sizes. One duct is 3.0 m in length and 0.3 m in each side width, and the other is 1.0 m in length and 0.1 m in each side width. Such ducts are easily found in HVAC engineering practice. The configuration of the computer applied is as follows: EMS memory is 4 GB, CPU is 3200 MHz and HD (hard disk) capacity is 500 G.

Because the velocity gradient becomes larger on the fluid approaching the duct wall, we refine the mesh there. The ducts in this study have two different working conditions: one has upward flow, and the other has downward flow. More details about the grid generation and duct position are presented in Fig. 1. Grid independence study is introduced in this paper. Nine kinds of grids with different grid number of 1×10^4, 5×10^4, 8×10^4, 1×10^5, 5×10^5, 8×10^5, 1×10^6, 5×10^6, and 8×10^6 are used to predict the dimensionless particle deposition velocity. The difference of the predicted results is found to be minor for grid number from 8×10^5 to 10^6. Furthermore, there is no difference between the predicted results with the grid number of 1×10^6, 5×10^6, 8×10^6. Hence in the present simulation, the grid number is 10^6.

3. Results and discussion

This paper has considered the effects of drag, lift force, gravity, Brownian diffusion, and turbulent diffusion on the dimensionless deposition velocity based on Reynolds-averaged Navier–Stokes (RANS)-Lagrangian simulation. The impact of gravity, lift force, particle density, duct size, air velocity, and turbulent flow development on dimensionless deposition velocity can be seen in Table 2. Before the discussion of those impact factors on dimensionless deposition velocity, simulation validation is introduced to make simulation results credibility.

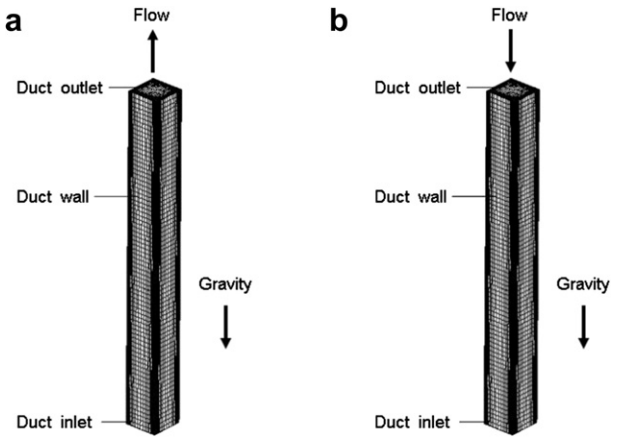

Fig. 1. Grid generation and duct position. (a) Duct with upward flow. (b) Duct with downward flow.

Table 2
The impact of gravity, lift force, particle density, duct size, air velocity, and turbulent flow development on dimensionless deposition velocity.

Impact factors	Particle deposition in downward flow		Particle deposition in upward flow	
	$5 < \tau^+ < 100$	$\tau^+ > 100$	$5 < \tau^+ < 100$	$\tau^+ > 100$
Gravity	(−)	+	(−)	−
Lift force	(−)	+	(−)	−
Particle density	(−)	(−)	(−)	(−)
Duct size	(−)	(−)	(−)	(−)
Air velocity	(−)	+	(−)	+
Turbulent flow development (from developing to developed)	(−)	−	(−)	−

τ^+ = Dimensionless relaxation time; (−) = no effect; + = positive effect; − = negative effect.

3.1. Simulation validation

The predicted dimensionless deposition velocity is compared with the experimental data collected by Liu and Agarwal (1974) [26], the DNS results predicted by Uigttewaal and Oliemans (1996) [7] and the RSM results predicted data of Jinping Zhang (2006) [4]. The comparison results are illustrated in Fig. 2.

For $5 < \tau^+ < 800$, the current predicted results well agree with previous studies of Liu and Agarwal (1974), Uijttewaal and Oliemans (1996) and Jinping Zhang (2006). For$\tau^+ > 800$, the predicted dimensionless deposition velocity in downward flow is larger than that in previous studies, while dimensionless deposition velocity in upward flow is smaller than that in previous studies. The reason is that the gravity of particles in vertical duct flow increase or decrease the lift force which will result in the change of dimensionless deposition velocity, see Section 3.3.

3.2. Effect of particle diameter on deposition velocity

The variation of dimensionless deposition velocity of particles ranging from 10 μm to 200 μm versus particle diameter at the air velocity of 7.0 m/s for fully developed downward or upward flow in vertical ducts based on RANS-Lagrangian model can be seen in Fig. 3. It can be observed that, for both downward and upward flow, dimensionless deposition velocity of particles whose diameter ranges from 10 to 50 μm increases obviously as particle diameter increases, and then decreases when particles size are between 50 and 100 μm. As particle diameter increases from 50 to 200 μm, dimensionless deposition velocity is larger in downward flow than upward flow. Meanwhile, the difference between the dimensionless deposition velocity in downward and upward flow becomes much more obvious as the particle diameter increases. This phenomenon can also be observed by studies [5,6].

In both upward flow and downward flow, the dimensionless deposition velocity of particle whose diameter ranges from 10 to 50 μm increases as particle diameter increases because, for particles in the diffusion-impaction regime, large particles in this regime can be obviously influenced by flows in the near-wall region which lead to more deposition. While for the particles whose diameter is larger than 50 μm, the velocity tends to decrease because the particles are too large to respond rapidly to the fluctuation of near-wall turbulent eddies.

Although the dimensionless deposition velocity of particles larger than 50 μm in both upward flow and downward flow should have maintained the downtrend constantly, the particle deposition velocities decrease smaller in downward flow than in upward flow due to the influence of Saffman lift force. Saffman lift force enhances the deposition in downward flow and weakens the deposition velocities in upward flow. Additionally, Saffman lift force is proportional to the cube of particle diameter, see Eq. (14). That is why the difference between the dimensionless deposition velocity in downward and upward flow became much more obvious as the particle diameter increases.

3.3. Effect of gravity and lift force on deposition velocity

To investigate the influence of lift force on particle deposition, the flow without lift forceis introduced in the simulation. It might be difficult to be realized in experiment but easy in simulation. The variation of dimensionless deposition velocity particles whose

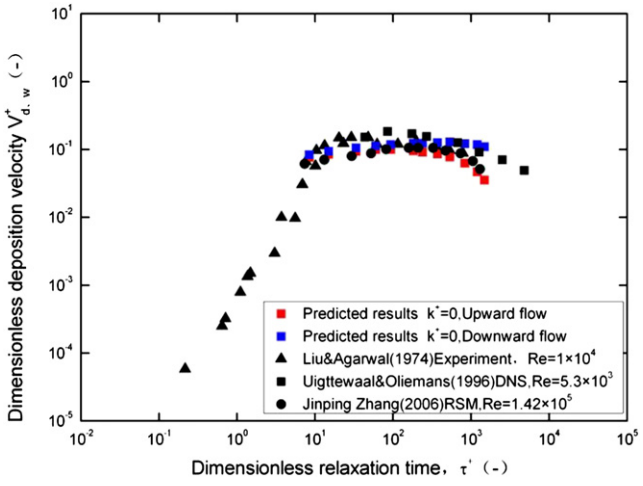

Fig. 2. Comparison of dimensionless wall deposition velocities predicted in a smooth vertical square ventilation duct with 30 cm × 30 cm cross-section with the data of Liu and Agarwal (1974), Uigttewaal and Oliemans (1996) and Jinping Zhang (2006).

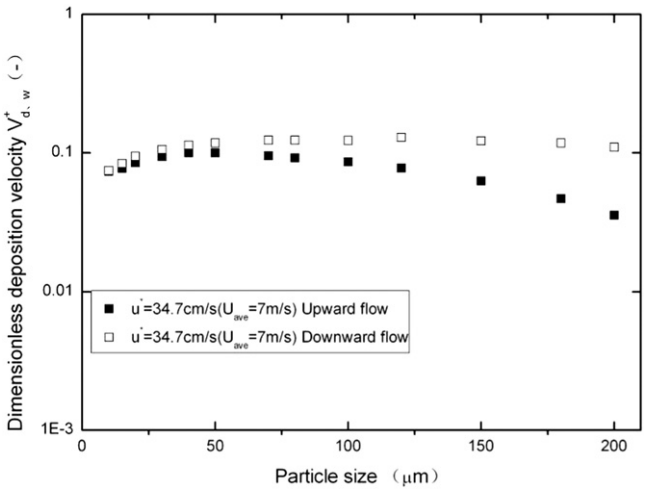

Fig. 3. Variation of dimensionless deposition velocity of particles ranging from 10 μm to 200 μm versus particle diameter at air velocity of 7.0 m/s for downward or upward flow.

diameter ranges from 10 to 200 μm versus dimensionless relaxation time in different flows can be seen in Fig. 4.

It can be observed that the influence of both gravity and lift force on deposition velocity is not obvious for $\tau^+ < 100$. While, for $\tau^+ > 100$, the influence becomes more obvious with τ^+ increases.

Gravity and lift force are proportional to d_p^3 and d_p^2 respectively, see Eqs. (13) and (14). The relationship between particle diameter and dimensionless relaxation time can be obtained from Eq. (22). Dimensionless relaxation time increases continuously while particle diameter increases. Thus for $\tau^+ < 100$, the particle diameter is so small that the gravity and lift force are much weaker than turbulent diffusion, drag, and Brownian diffusion. While for $\tau^+ > 100$, as the particle diameter increases, the influence of gravity and lift force becomes more important and eventually dominates the particle deposition process.

Based on Fig. 4, the dimensionless deposition velocity of particle is higher in downward flow than that in upward flow. This can be partially attributed to the effect of particle gravity. In vertical ducts, the direction of the gravity and the flow is parallel. So the gravity of particles will accelerate or decelerate particle velocity in the vertical direction which might lead to relative velocity between the particle and the fluid, and this relative velocity will affect Saffman lift force. In conclusion, gravity will not change dimensionless deposition velocity directly, and it is the Saffman lift force that changes the dimensionless deposition velocity.

Considering Saffman lift force, for $\tau^+ > 100$, the following phenomenon can be observed from Fig. 4:

(1) for downward flow, Saffman lift force increase the dimensionless particle deposition velocity;
(2) for upward flow, it decrease the velocity.

These phenomenons are due to the direction of Saffman lift force. As is known, the direction of the lift force depends on the relative stream-wise velocity between the particle and air. A particle in a velocity gradient near a wall (where du/dy is positive) with a stream-wise velocity higher than the air velocity will experience a negative lift force towards the wall, while a particle that lags the air stream in the stream-wise direction has a lift force away from the wall. For the downward flow, the gravity of the particle accelerates the stream-wise particle velocity, and thus generates the lift force towards the wall which increases the dimensionless deposition velocity. However, for the upward flow, the gravity decelerates the stream-wise particle velocity, and thus causes the lift force away from the wall which decreases the dimensionless deposition velocity of the particle.

3.4. Effect of particle density and duct size on particle deposition

In order to understand the effect of particle density and duct size on particle deposition based on Lagrangian simulation, two kinds of particle whose averaged density is 1800 kg/m^3 or 800 kg/m^3, and two kinds of the duct whose size is 0.3 m × 0.3 m × 3 m or 0.1 m × 0.1 m × 1 m are used in the simulation. The variation of the dimensionless deposition velocity V_d of particles versus dimensionless relaxation time is presented in Fig. 5.

It can be observed that, as dimensionless relaxation time increases, the three curves under different particle densities and duct size coincide with each other in the upward flow, and the same phenomenon can also be found in the downward flow, see Fig. 5. Particle density and duct size have no obvious influence on the dimensionless deposition velocity of particles.

3.5. Effect of friction velocity (air velocity) on deposition velocity

The variation of dimensionless deposition velocity versus dimensionless relaxation time in duct flow with fully developed velocity profiles at two air velocities of 3.0 m/s and 7.0 m/s based on RANS-Lagrangian model can be seen in Fig. 6.

Two observations can be drawn from Fig. 6. First, regardless of whether in upward flow or downward flow, particle deposition velocity at air velocity of 7.0 m/s tends to be higher than that at air velocity of 3.0 m/s, and this difference becomes more and more obvious as the dimensionless relaxation time increases. Second, for the downward flow, the particle deposition velocity at air velocity of 7.0 m/s is slightly higher than that at air velocity of 3.0 m/s. However, for upward flow, the difference is obvious, especially for $\tau^+ > 100$. In this case, particle deposition velocity at air velocity of 7.0 m/s is much higher than that at air velocity of 3.0 m/s. Simulated deposition velocities increase with increasing Reynolds number at high relaxation times because these particles are so large that their motion is not obviously influenced by flows in the near-wall region.

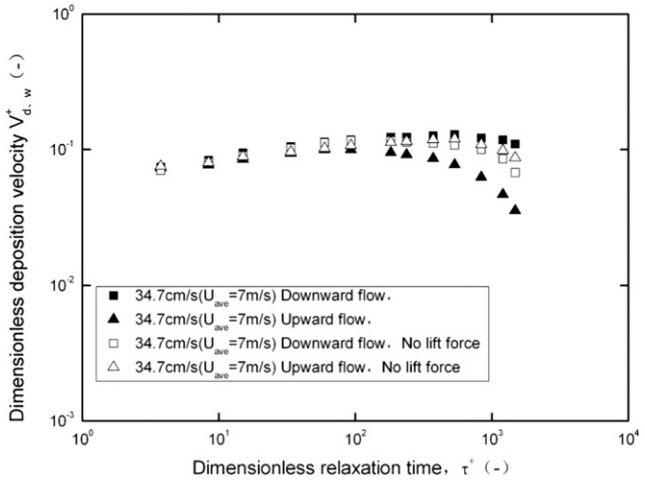

Fig. 4. Variation of dimensionless deposition velocity ranging from 10 to 200 μm versus dimensionless relaxation time in different flows.

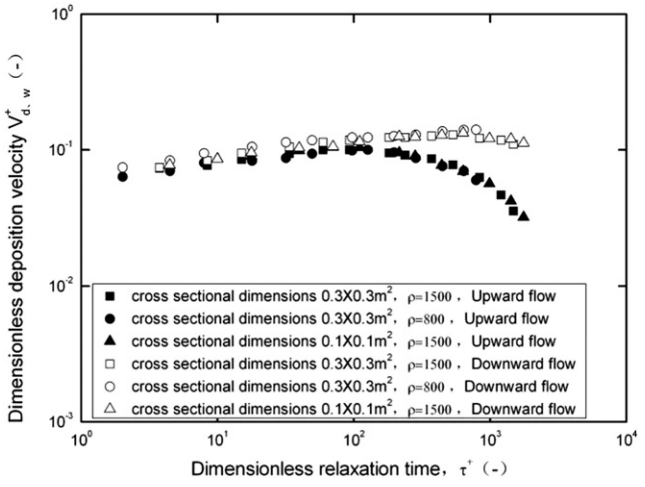

Fig. 5. Comparison of dimensionless floor deposition velocities predicted in a smooth vertical square ventilation duct with 30 cm × 30 cm and 10 cm × 10 cm cross-section with the particle density of 1800 kg/m^3 and 800 kg/m^3.

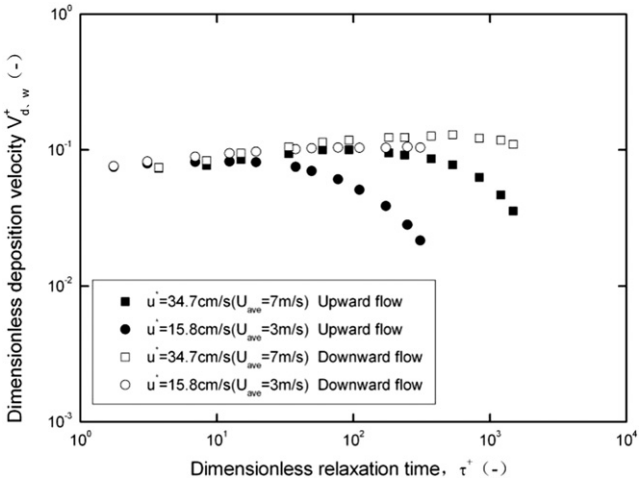

Fig. 6. Variation of dimensionless deposition velocity versus dimensionless relaxation time in duct flow with fully developed velocity profiles at two air velocities of 3.0 m/s and 7.0 m/s.

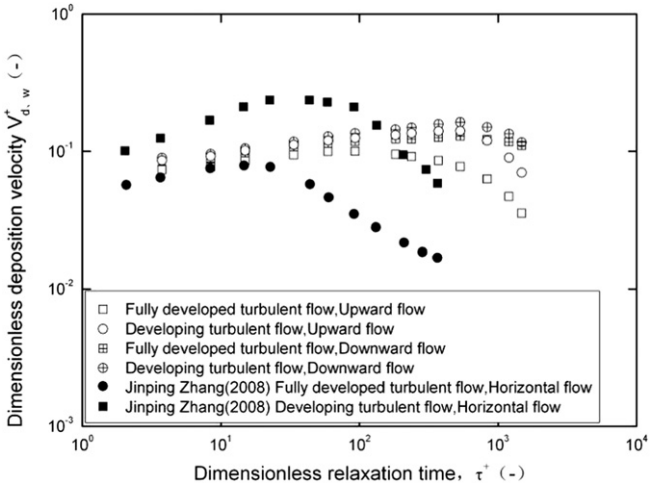

Fig. 7. Prediction dimensionless deposition velocity of turbulent flow with fully developed or developing velocity profiles.

3.6. *Effect of turbulent flow development on particle deposition*

In HVAC systems, there are duct flows with fully developed velocity profiles and developing velocity profiles. In order to understand the effect of turbulent flow on particle deposition, dimensionless particle deposition velocities on the duct surface in upward and downward flow with developing velocity profiles are predicted by RANS-Lagrangian simulation.

Predicted dimensionless deposition velocity in upward or downward duct flow with developing velocity profiles is compared with the fully developed velocity profiles at air velocity of 7.0 m/s in Fig. 7.

For $5 < \tau^+ < 100$, no matter the particles are in upward flow or downward flow, the dimensionless deposition velocities of particles in vertical duct flow with developing velocity profile is slightly higher than that in vertical duct with fully developed velocity profile, while for $\tau^+ > 100$, the difference of the two deposition velocities in vertical duct flow with different turbulent development is obvious, especially in upward flow. It should be noticed when the dimensionless relaxation time is about 800, the influence of turbulent development on particle deposition tend to decrease slightly.

For $5 < \tau^+ < 100$, turbulent diffusion is the dominant transport mechanism. Because the turbulent intensity of duct flow with developing velocity profiles is greater than that of duct flow with fully developed velocity profiles, the dimensionless deposition velocity is higher in the former flow than in the latter.

The air velocity in the near-wall region in the duct flow with developing velocity profiles, which is at the inlet of the duct, is lower than that in duct flow with fully developed velocity profiles, see Fig. 8. Since the particles are released at the inlet with the same velocity, lower velocity in the near-wall region means higher relative velocity between particle and air, thus affects the Saffman lift force. For the upward flow, it will increase the relative velocity between the particle and the air in the axial direction, and thus increases the Saffman lift force towards the wall. While for downward flow, it will decrease the relative velocity between the particle and the air which decreases the lift force away from the wall. Both effects lead to the higher dimensionless deposition velocity, see equation [13]. Furthermore, the lift force is proportional to d_p^2, for $\tau^+ < 100$, the particle diameter is so small that the gravity and lift force are much weaker than turbulent diffusion, drag. While for $\tau^+ > 100$, as the particle diameter increases to certain extent, the influence of gravity and lift force becomes more important and eventually dominates the particle deposition process. In addition, the same change tendency can be observed in the data from Jinping

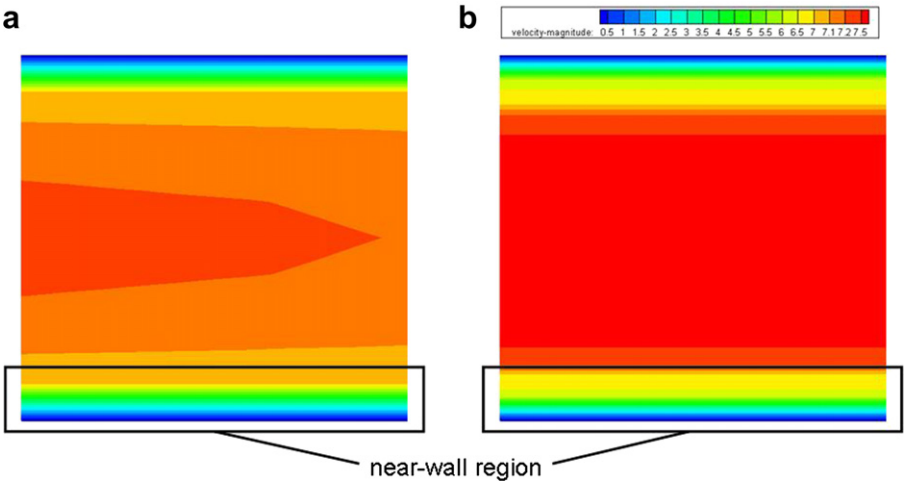

Fig. 8. Difference between the developing velocity profiles and fully developed velocity profiles. (a) developing velocity profiles, (b) fully developed velocity profiles.

Zhang (2008) in a horizontal duct between fully developed turbulent flow and developing turbulent flow.

4. Conclusions

Considering the effects of drag, lift force, gravity, Brownian diffusion, and turbulent diffusion on the dimensionless deposition velocity of particles on vertical duct surfaces using fully developed and developing velocity profiles. Based on the Reynolds stress transport model (RSM) at two different air velocities, 3.0 m/s and 7.0 m/s, the aforementioned effects were predicted using Reynolds-averaged Navier–Stokes (RANS)-Lagrangian simulation on square shaped ducts under vertical flows. Results from this study provide some new guidelines in particle deposition mechanism, as well as contribute to the discussion on interaction of gravity and lift force. The main conclusions are as follows:

In both upward flow and downward flow, the dimensionless deposition velocity of particle whose diameter ranges from 10 to 50 μm increases as particle diameter increases because of the interaction of turbulent eddies. While for the particles whose diameter is larger than 50 μm, the velocity decrease because the particles are too large to respond rapidly to the fluctuation of near-wall turbulent eddies. Meanwhile, the difference between the dimensionless deposition velocity in downward and upward flow becomes much more obvious as the particle diameter increases from 50 to 200 μm.

For $\tau^+ > 100$, both the influence of gravity and lift force are important for particle deposition. Gravity of particles will accelerate or decelerate particle velocity in the axial direction and thus lead to greater relative velocity between the particle and the air. For the downward flow, the gravity accelerates the stream-wise particle velocity, and thus enhances the lift force towards the duct wall that increases the dimensionless deposition velocity. While, for the upward flow, the gravity decelerates the stream-wise particle velocity, and thus causes the lift force away from the wall which decreases the dimensionless particle deposition velocity.

Particle deposition velocity at air velocity of 7.0 m/s is higher than that at air velocity of 3.0 m/s, and the difference becomes more and more obvious as the dimensionless relaxation time increases. For the downward flow, the particle deposition at air velocity of 7.0 m/s has no obvious difference from that of 3.0 m/s, and the former is higher than the latter. However, for the upward flow, the difference is obvious, especially for $\tau^+ > 100$. This phenomenon can be summarized as that deposition velocities increase with increasing Reynolds number at high relaxation times. Those particles are so large that their motions can not be obviously influenced by flows in the near-wall region.

In both upward flow and downward flow, the particle density and duct size have no obvious influence on the dimensionless deposition velocity of particles.

For $5 < \tau^+ < 100$, no matter the particles are in upward flow or downward flow, the dimensionless deposition velocities of particles in vertical duct flow with developing velocity profile is higher than that with fully developed velocity profile, while for $\tau^+ > 100$, the difference of the two deposition velocities in vertical duct flow with different turbulent development is obvious, especially in upward flow.

Acknowledgements

This research project is sponsored by Natural Science Foundation of China (No.50878177, No.50778145) and Key Projects in the National Science & Technology Pillar Program during the Eleventh Five-Year Plan Period in China (2008BAJ08B07, 2006BAJ02A10).

References

[1] Wallin O. PhD dissertation. Stockholm, SwedenRoyal: Institute of Technology; 1994.
[2] Zuraimia MS, Weschlerb CJ, Thama KW, Fadeyia MO. The impact of building recirculation rates on secondary organic aerosols generated by indoor chemistry. Atmospheric Environment 2007;41:5213–23.
[3] Liu Chaosheng, Ahmadi Goodarz. Transport and deposition of particles near a building model. Building and Environment 2006;41:828–36.
[4] Zhang Jinping. Numerical simulation and experimental study on particle deposition in ventilation ducts. PhD Thesis. School of Environmental and Municipal Engineering, Xi' an, Shaanxi: Xi'an University of Architecture and Technology; 2006.
[5] Zhang Jinping, Li Angui, Li Desheng. Modeling deposition of particles in typical horizontal ventilation duct flows. Energy Conversion and Management 2008;49:3672–83.
[6] Zhang Jinping, Li Angui. CFD simulation of particle deposition in a horizontal turbulent duct flow. Chemical Engineering Research and Design 2008;86: 95–106.
[7] Uijttewaal WSJ, Oliemans RVA. Particle dispersion and deposition in direct numerical and large eddy simulations of vertical pipe flows. Physics of Fluids 1996;8:2590–604.
[8] Zhang H, Ahmadi G. Aerosol particle transport and deposition in vertical and horizontal turbulent duct flows. Journal of Fluid Mechanics 2000;406:55–80.
[9] Brooke JW, Kontomaris K, Hanratty TJ, McLaughlin JB. Turbulent deposition and trapping of aerosols at a wall. Physics of Fluids A 1992;4(4):825–34.
[10] McLaughlin JB. Aerosol particle deposition in numerically simulated channel flow. Physics of Fluids A 1989;1(7):1211–24.
[11] Zhang Z, Chen Q. Prediction of particle deposition onto indoor surfaces by CFD with a modified Lagrangian method. Atmospheric Environment 2009;43: 319–28.
[12] Lo lacono Giovanni, Andrew M, Reynolds A. Lagrangian stochastic model for the dispersion and deposition of Brownian particles in the presence of a temperature gradient. Aerosol Science 2005;36:1238–50.
[13] Chen Fangzhi, Alvin C, Lai K. An Eulerian model for particle deposition under electrostatic and turbulent conditions. Aerosol Science 2004;35:47–62.
[14] Hryb D, Cardozo M, Ferro S, Goldschmit M. Particle transport in turbulent flowusing both Lagrangian and Eulerian formulations. International Communications in Heat and Mass Transfer 2009;36:451–7.
[15] Saffman PG. The lift on a small sphere in a slow shear flow. Journal of Fluid Mechanics 1965;22:385–400.
[16] Saffman PG. Corrigendum to the lift on a small sphere in a slow shear flow. Journal of Fluid Mechanics 1968;31:624.
[17] Daly BJ, Harlow FH. Transport equations in turbulence. Physics of Fluids 1970;13:2634–49.
[18] Fu S, Launder BE, Leschziner MA. Modeling Strongly Swirling Recirculating Jet Flow with Reynolds-Stress Transport Closures. In: Sixth Symposium on Turbulent Shear Flows, Toulouse, France; 1987.
[19] Lien FS, Leschziner MA. Assessment of turbulent transport models including non-linear RNG eddy – viscosity formulation and second-moment closure. Computers and Fluids 1994;23(8):983–1004.
[20] Fluent. Fluent user's guide, version 6.1. NH, USA: Fluent Inc.; 2003.
[21] Graham DI, James PW. Turbulent dispersion of particles using eddy interaction models. International Journal of Multiphase Flow 1996;22:157–75.
[22] Morsi SA, Alexander AJ. An investigation of particle trajectories in two-phase flow systems. Journal of Fluid Mechanics 1972;55:193–208.
[23] Anand N., McFarland AR, Wong FS, Kocmoud CJ. Deposition: software to calculate particle penetration through aerosol transport lines, NUREG/GR-0006, U.S.NRC Final Report, 1993.
[24] White FM. Fluid mechanics. 2nd ed. NewYork: McGraw-Hill; 1986.
[25] Wu Jun, Zhao Bin. Effect of ventilation duct as a particle filter. Building and Environment 2007;42:2523–9.
[26] Liu BYH, Agarwal JK. Experimental observation of aerosol deposition in turbulent flow. Aerosol Science 1974;5:145–55.